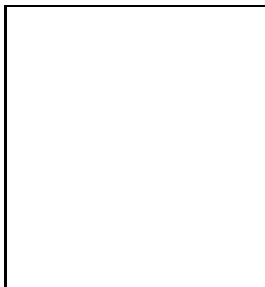


BELLE NEW RESULTS ON $B \rightarrow D^{**}\ell\nu$ DECAYS

D. LIVENTSEV

*Institute for Theoretical and Experimental Physics,
B. Cheremushkinskaya, 25, 117218 Moscow, Russia
(For the Belle collaboration)*



We present a study of semileptonic B decays to P -wave D^{**} mesons at Belle. Semileptonic decay to a D_2^* meson is observed for the first time and its product branching ratio is measured to be $\mathcal{B}(B^+ \rightarrow \bar{D}_2^{*0}\ell^+\nu) \times \mathcal{B}(\bar{D}_2^{*0} \rightarrow D^-\pi^+) = 0.22 \pm 0.03(\text{stat.}) \pm 0.04(\text{syst.})\%$.

1 Introduction

Heavy Quark Effective Theory (HQET) has proven to be very successful at describing semileptonic decays of B -mesons, especially inclusive transitions. However, some difficulties arise when it is applied to exclusive decays. For example, certain sum rules (in particular, the Uraltsev sum rule¹) imply the strong dominance of decays to the narrow excited D mesons over those to the wide ones, while some experimental data show the opposite trend^{2,3}. However, no complete experimental study of such semileptonic decays to excited D mesons exists, and thus no direct comparison with theoretical predictions can be performed. Here we present Belle study of $B \rightarrow D^{(*)}\pi\ell\nu$ decays and measurement of the excited D contributions to the $D^{(*)}\pi$ final state⁴.

According to HQET there are two doublets of orbitally excited (P -wave) charmed mesons (D^{**}), differentiated by their light quark angular momentum $j_q = 1/2$ or $j_q = 3/2$. Members of the $j_q = 3/2$ doublet are predicted to decay only via a D -wave and be relatively narrow, while members of the $j_q = 1/2$ doublet are predicted to decay only via an S -wave and be relatively broad⁵. The D^{**} states with spin-parity and light quark angular momentum combinations $0^+(j_q = 1/2)$, $1^+(j_q = 1/2)$, $1^+(j_q = 3/2)$ and $2^+(j_q = 3/2)$ are usually labelled D_0^* , D_1' , D_1 and D_2^* , respectively. The D^{**} states have previously been observed and studied in hadronic B decays⁶. Semileptonic B decays to narrow D_1 and D_2^* mesons have been studied by a number of experiments⁷. The semileptonic branching fractions of $B \rightarrow D^{(*)}\pi\ell\nu$ decays were measured by Belle⁸ and BaBar⁹.

This measurement is based on a data sample that contains 657 million $B\bar{B}$ pairs, which corresponds to 605 fb^{-1} , collected at the $\Upsilon(4S)$ resonance with the Belle detector¹¹ operating at the KEKB asymmetric-energy e^+e^- collider¹⁰. An additional 68 fb^{-1} data sample taken at a center-of-mass energy 60 MeV below the $\Upsilon(4S)$ resonance is used to study continuum $e^+e^- \rightarrow q\bar{q}$ ($q = u, d, s, c$) background.

2 Data analysis

To suppress the large combinatorial background expected in the reconstruction of final states including a neutrino, we use a full reconstruction tagging method. The first B meson (denoted as B_{sl}) is reconstructed in the semileptonic mode of interest, *i.e.* as a combination of all final particles $D^{(*)}\pi\ell$ except for the neutrino. The remainder of the event is combined into either a $D^{(*)}\pi\pi^\pm$ ($n \leq 6$) or $D^{(*)}\rho^-$ combination to form the tagging B meson (referred to below as B_{tag}). Semileptonic decays are identified by a peak around zero in the missing mass squared spectrum, $M_\nu^2 = (P_{\text{beams}} - P_{\text{tag}} - P_{\text{sl}})^2$, where P_{beams} is the total four-momentum of the beams and P_{tag} and P_{sl} are the reconstructed four-momenta of the B_{sl} and B_{tag} , respectively. This method provides significantly improved resolution in the missing momentum in comparison with non-tagging methods, thus allowing background suppression, separation of different decay modes and precise calculation of the decay kinematics. The M_ν^2 spectra for the four semileptonic decays $B \rightarrow D^{(*)}\pi\ell\nu$ are shown in Figs. 1, *1a)–1d*) as points with error bars.

We divide the backgrounds into the following categories: (1) Continuum, (2) Backgrounds with the B_{tag} misreconstructed from particles belonging to the other B meson or fake tracks, (3) B_{sl} backgrounds with the B_{tag} reconstructed correctly, which can be further separated by their source: (3a) Combinatorial background under the $D^{(*)}$ signal from B_{sl} , (3b) Hadrons misidentified as leptons, (3c) Feed-down from $B \rightarrow D^*\pi\ell\nu$ reconstructed as $B \rightarrow D\pi\ell\nu$ with lost neutral(s). All backgrounds except for (3c) are reliably determined and finally subtracted directly from the data. Background (3c) is observed only in the $B \rightarrow D\pi\ell\nu$ channels and is estimated from a Monte Carlo (MC) simulation with normalization fixed to the data using $B \rightarrow D^*(\pi)\ell\nu$ signal yields. This contribution is plotted in Figs. 1, *1a), 1c*) as open histograms.

The background-subtracted M_ν^2 distributions are shown in Figs. 1, *2a)–2d*). These distributions are fitted with signal functions, the shapes of which are fixed from MC studies. Fitted signal yields, reconstruction efficiencies and branching ratios are summarized in Table 1. The branching ratios are calculated relative to the normalization modes $B \rightarrow D\ell\nu$ to cancel out the B_{tag} reconstruction efficiency according to the formula: $\mathcal{B}(\text{mode}) = \mathcal{B}(\text{norm}) \times N_{\text{mode}}/N_{\text{norm}} \times \epsilon_{\text{norm}}/\epsilon_{\text{mode}}$, where $N_{\text{norm(mode)}}$ and $\epsilon_{\text{norm(mode)}}$ are the signal yield and reconstruction efficiency of the normalization mode (mode of interest) and the normalization mode \mathcal{B} is taken from the PDG¹². Relative efficiencies are obtained from MC simulation. Intermediate branching fractions are included, while the tagging efficiency is not. The reconstruction and background subtraction procedures for the $B \rightarrow D\ell\nu$ mode are identical to those applied for the studied channels. The obtained branching fractions are in good agreement with our previous measurement⁸ and with BaBar results⁹.

Signals for semileptonic B decays to orbitally excited D^{**} are extracted from the $D^{(*)}\pi$ invariant mass distributions. We define a signal window for $B \rightarrow D^{(*)}\pi\ell\nu$ decays by the requirement $|M_\nu^2| < 0.1\text{ GeV}^2/c^4$. The backgrounds are estimated in the same way as in the M_ν^2 distribution study. The $D^{(*)}\pi$ invariant mass spectra from the signal window after subtraction of backgrounds (1-3) are shown in Fig. 2. The mass distributions before background subtraction, restricted to the region near the $j_q = 3/2$ states, are shown in the insets.

To extract the D^{**} signals we perform simultaneous unbinned likelihood fits to the signal and background $D^{(*)}\pi$ mass spectra. The signal function includes all orbitally excited D^{**} contributing to the given final state (D_0 and D_2^* to $D\pi$ and D_1, D_1', D_2^* to $D^*\pi$), each of

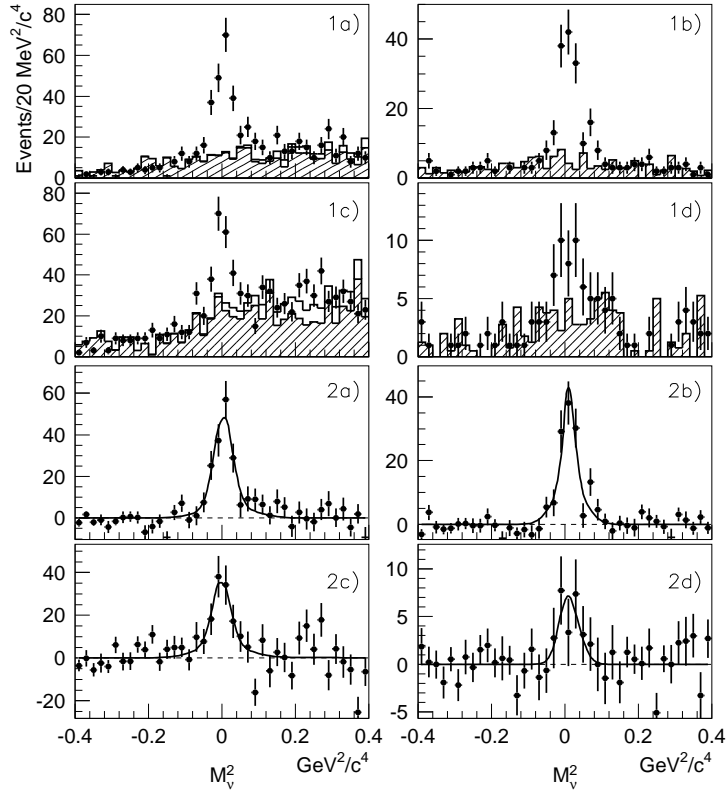


Figure 1: M_ν^2 spectra before (1) and after (2) background subtraction for: a) $B^+ \rightarrow D^- \pi^+ \ell^+ \nu$, b) $B^+ \rightarrow D^{*-} \pi^+ \ell^+ \nu$, c) $B^0 \rightarrow \bar{D}^0 \pi^- \ell^+ \nu$, d) $B^0 \rightarrow \bar{D}^{*0} \pi^- \ell^+ \nu$. The curves are the fits, which are described in the text.

which is described by a relativistic Breit-Wigner function for a known orbital momenta, and a non-resonant part described by the Goity-Roberts model¹⁴. D^{**} masses and widths are fixed to measured values⁶. To further investigate the $D\pi$ mass spectrum we also test a $D_v^* + D_2^*$ hypothesis. Despite the $D^0\pi^+$ mass region corresponding to D^{*+} being excluded from the study, and while D^{*0} is below the $D^-\pi^+$ threshold, a virtual D_v^* can be produced off-shell. We describe the D_v^* contribution by a tail of the Breit-Wigner function with floating normalization. Fit results are shown as a dashed line for this combination.

Fitted resonance yields and corresponding product branching ratios are listed in Table 2. The contribution of the non-resonant component in all cases is consistent with zero. The $B \rightarrow D^{**} \ell \nu$ decay significance is defined as $\sqrt{-2 \ln L_{\max}/L_0}$, where L_0 is the likelihood value returned by the fit to the $D^{(*)}\pi$ distribution with the D^{**} contribution fixed to zero. Our result for $B \rightarrow \bar{D}_1 \ell^+ \nu$ is in good agreement with previous measurements⁷. For a $D_0^* + D_2^*$ hypothesis the branching

Table 1: Results for $B \rightarrow D^{(*)}\pi\ell\nu$ where the first error is statistical and the second is systematic.

Mode	Yield	Eff.,%	$\mathcal{B}(\text{mode}),\%$
$B^+ \rightarrow \bar{D}^0 \ell^+ \nu$	2320 ± 60	6.4	2.15 ± 0.22^{13}
$B^+ \rightarrow D^- \pi^+ \ell^+ \nu$	192 ± 19	2.8	$0.40 \pm 0.04 \pm 0.06$
$B^+ \rightarrow D^{*-} \pi^+ \ell^+ \nu$	123 ± 14	1.14	$0.64 \pm 0.08 \pm 0.09$
$B^0 \rightarrow D^- \ell^+ \nu$	760 ± 30	3.7	2.12 ± 0.20^{13}
$B^0 \rightarrow \bar{D}^0 \pi^- \ell^+ \nu$	150 ± 20	3.7	$0.42 \pm 0.07 \pm 0.06$
$B^0 \rightarrow \bar{D}^{*0} \pi^- \ell^+ \nu$	22 ± 8	0.40	$0.56 \pm 0.21 \pm 0.08$

ratio of the decay to the wide D_0^* is large, in contrast to theoretical predictions³. However, the present statistics do not definitely exclude an interpretation of broadly distributed $D\pi^+$ events as the D_v^* tail.

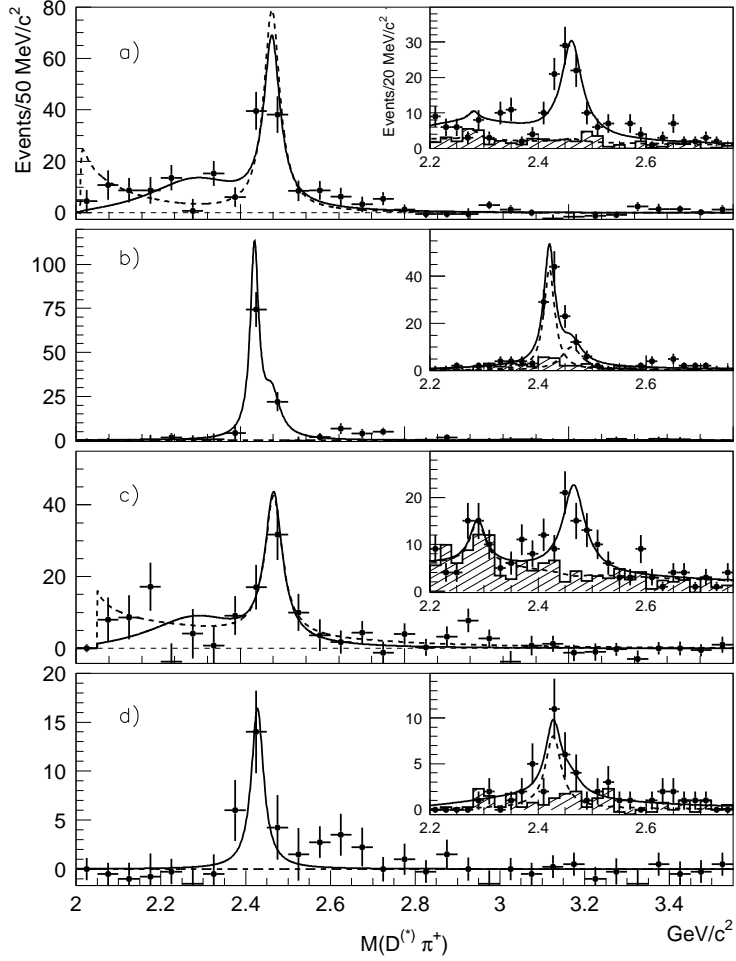


Figure 2: Hadronic invariant mass distributions for: a) $B^+ \rightarrow D^- \pi^+ \ell^+ \nu$, b) $B^+ \rightarrow D^{*-} \pi^+ \ell^+ \nu$, c) $B^0 \rightarrow \bar{D}^0 \pi^- \ell^+ \nu$, d) $B^0 \rightarrow \bar{D}^{*0} \pi^- \ell^+ \nu$. Insets show the distributions before background subtraction in the region around the narrow D^{**} 's. The background is shown as the hatched histogram. The curves are the fits, which are described in the text.

For $D^{*,**}$'s decaying into $D\pi$ we perform a study of the helicity angle distributions, which is the angle between π momentum and the direction opposite to B_{sl} -momentum in the $D^{*,**}$ rest frame. To extract the D_v^* , D_0^* and the D_2^* helicity distributions we perform a combined fit of the $M(D\pi)$ spectra for $D\pi$ combinations from both B^+ and B^0 in bins of helicity angle. The fit procedure is identical to that used for the $\mathcal{B}(B \rightarrow D^{*,**} \ell \nu)$ calculation. The results corrected for the efficiency are plotted in Fig. 3. D_2^* distributions for D_v^* and D_0^* hypothesis coincide within errors, so that only that for the $D_0^* + D_2^*$ case is shown in Fig. 3 c. The D_0^* helicity distribution is consistent with the $J = 0$ hypothesis ($\chi^2/ndf = 6.0/4$, where ndf is the number of degrees of freedom). The D_2^* helicity distribution is fitted with the function $a_0^2 |Y_2^0|^2 + 4a_1^2 |Y_2^1|^2 + 4a_2^2 |Y_2^2|^2$, where the Y_j^i are spherical harmonics and $a_0^2 + 4a_1^2 + 4a_2^2 = 1$. The fit yields $a_0^2 = 0.74 \pm 0.10$, $a_1^2 = 0.04 \pm 0.02$ and $a_2^2 = 0.02 \pm 0.02$; the fit quality is $\chi^2/ndf = 2.0/3$. The fit is consistent with the assumed quantum numbers and demonstrates that the D_2^* from semileptonic decay is dominantly in the $s_z = 0$ spin projection. Helicity distributions, predicted by theory, are shown as dashed lines. For evaluating the $D_v^* + D_2^*$ hypothesis, the obtained D_v^* helicity distribution (Fig. 3 b) is fitted with the function $b_0^2 |Y_1^0|^2 + b_1^2 |Y_1^1|^2$. This fit yields

Table 2: Results of the $D^{(*)}\pi^+$ pair invariant mass study. $\mathcal{B}(\text{mode}) \equiv \mathcal{B}(B \rightarrow D^{**}\ell\nu) \times \mathcal{B}(D^{**} \rightarrow D^{(*)}\pi^+)$. The first error is statistical and the second is systematic.

Mode	Yield	$\mathcal{B}(\text{mode}),\%$	Signif.
$B^+ \rightarrow \bar{D}_0^{*0}\ell^+\nu$	102 ± 19	$0.24 \pm 0.04 \pm 0.06$	5.4
$B^+ \rightarrow \bar{D}_2^{*0}\ell^+\nu$	94 ± 13	$0.22 \pm 0.03 \pm 0.04$	8.0
$B^0 \rightarrow D_0^{*-}\ell^+\nu$	61 ± 22	$0.20 \pm 0.07 \pm 0.05$	2.6
		< 0.4 @ 90% C.L.	
$B^0 \rightarrow D_2^{*-}\ell^+\nu$	68 ± 13	$0.22 \pm 0.04 \pm 0.04$	5.5
$B^+ \rightarrow \bar{D}_1^{\prime 0}\ell^+\nu$	-5 ± 11	< 0.07 @ 90% C.L.	
$B^+ \rightarrow \bar{D}_1^0\ell^+\nu$	81 ± 13	$0.42 \pm 0.07 \pm 0.07$	6.7
$B^+ \rightarrow \bar{D}_2^{\prime 0}\ell^+\nu$	35 ± 11	$0.18 \pm 0.06 \pm 0.03$	3.2
$B^0 \rightarrow D_1^{\prime -}\ell^+\nu$	4 ± 8	< 0.5 @ 90% C.L.	
$B^0 \rightarrow D_1^-\ell^+\nu$	20 ± 7	$0.54 \pm 0.19 \pm 0.09$	2.9
		< 0.9 @ 90% C.L.	
$B^0 \rightarrow D_2^{*-}\ell^+\nu$	1 ± 6	< 0.3 @ 90% C.L.	

$b_0^2 = 0.15 \pm 0.09$, $b_1^2 = 0.85 \pm 0.09$ ($\chi^2/ndf = 18.8/4$) in poor agreement with expectations from theory, shown as a dashed line.

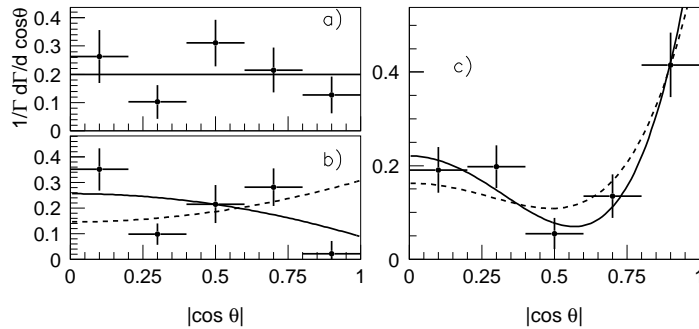


Figure 3: Helicity distributions for a) D_0^* , b) D_v^* , c) D_2^* . The curves represent the fits, described in the text.

We also study the dependence of the $B \rightarrow D^{**}$ transition on q^2 or, equivalently, on the conventional HQET variable w , which is the dot-product of B and D^{**} four-velocities: $w = v_B \cdot v_{D^{**}}$. The w -dependence is obtained from fits of $D\pi$ invariant mass in bins of w . The results are presented in Fig. 4. As with the helicity study the D_2^* distribution is shown only for the $D_0^* + D_2^*$ hypothesis in Fig. 4 c. The w distribution is fitted according to the model given in Ref. ¹⁵. In HQET, the matrix elements between the B and D states to leading order in Λ_{QCD}/m_Q are expressed in terms of three universal Isgur-Wise functions $\xi(w)$, $\tau_{1/2}(w)$ and $\tau_{3/2}(w)$ for (D, D^*) , (D_0^*, D_1^*) and (D_1, D_2^*) doublets, respectively ¹⁵. We assume a ‘‘pole’’ form for $\xi(w)$: $\xi = (2/(1+w))^{2\rho^2}$ and a linear form for $\tau_i(w)$ functions: $\tau_i(w) = \tau_i(1)[1 + \hat{\tau}'_i(w-1)]$, and the following relation: $\hat{\tau}'_{1/2} = \hat{\tau}'_{3/2} + 0.5$ ¹⁶. A simultaneous fit to the w -distributions for D_0^* and D_2^* gives $\hat{\tau}'_{3/2} = -1.8 \pm 0.3$. Using the measured branching ratios of $B \rightarrow D_{0,2}^*\ell\nu$, we also calculate $\tau_{3/2}(1) = 0.75$ and $\tau_{1/2}(1) = 1.28$. All parameters are in agreement with expectations except for $\tau_{1/2}(1)$, which is larger than predicted due to the large value of $\mathcal{B}(B \rightarrow D_0^*\ell\nu)$.

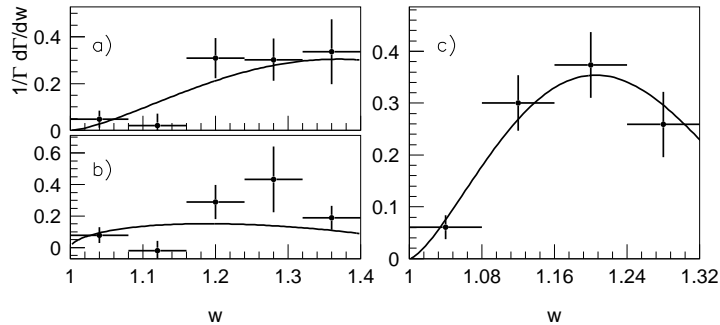


Figure 4: w distributions for a) D_0^* , b) D_v^* , c) D_2^* . The curves are the fits, which are described in the text.

3 Conclusion

In conclusion, we measured the branching fractions for $B \rightarrow D^{(*)}\pi\ell\nu$ decays. We also performed an analysis of the final state $D^{(*)}\pi$ hadronic system and obtained branching ratios for the $B \rightarrow D^{**}\ell\nu$ components. Semileptonic decay to D_2^* meson is observed and measured for the first time. Helicity and w distributions are studied for this decay. We observe a broad enhancement in the $D\pi$ mass distribution consistent with wide D_0^* production. The branching ratio of the decay to $B \rightarrow D_0^*\ell\nu$ is found to be large, in contrast with theoretical predictions³. However there is no indication of a broad D_1' in the $B \rightarrow D^*\pi\ell\nu$ channel, which should be of the same order. The combined likelihood of fits to the $D\pi$ mass, helicity and w distributions for $D_0^* + D_2^*$ hypothesis is higher than that for the $D_v^* + D_2^*$ combination by 2.8σ . However, the present data sample cannot exclude the interpretation of this enhancement as a D_v^* tail.

References

1. N. Uraltsev, Phys. Lett. B **501**, 86 (2001).
2. N. Uraltsev, hep-ph/0409125.
3. I.I. Bigi *et al.*, Eur. Phys. J. C **52**, 975 (2007).
4. D. Liventsev *et al.* (Belle Collaboration), Phys. Rev. D **77**, 091503 (2008).
5. J. Rosner, Comm. Nucl. Part. Phys. **16**, 109 (1986).
6. K. Abe *et al.* (Belle Collaboration), Phys. Rev. D **69**, 112002 (2004); A. Kuzmin *et al.* (Belle Collaboration), Phys. Rev. D **76**, 012006 (2007).
7. D. Buskulic *et al.* (ALEPH Collaboration), Z. Phys. C **73**, 601 (1997); A. Anastassov *et al.* (CLEO Collaboration), Phys. Rev. Lett. **80**, 4127 (1998); V.M. Abazov *et al.* (D0 Collaboration), Phys. Rev. Lett. **95**, 171803 (2005); J. Abdallah *et al.* (DELPHI Collaboration), Eur. Phys. J. C **45**, 35 (2006).
8. D. Liventsev *et al.* (Belle Collaboration), Phys. Rev. D **72**, 051109 (2005).
9. B. Aubert *et al.* (BaBar Collaboration), arXiv:0708.1738.
10. S. Kurokawa and E. Kikutani, Nucl. Instr. and Meth. A **499**, 1 (2003), and other papers included in this volume.
11. A. Abashian *et al.* (Belle Collaboration), Nucl. Instr. and Meth. A **479**, 117 (2002).
12. W.-M. Yao *et al.* (Particle Data Group), J. Phys. G **33**, 1 (2006).
13. Used as a reference.
14. J.L. Goity, W. Roberts, Phys. Rev. D **51**, 3459 (1995).
15. A. Le Yaouanc *et al.*, Phys. Lett. B **520**, 25 (2001).
16. S. Veseli, M.G. Olsson, Phys. Lett. B **367**, 302 (1996).